Oncostatin M-induced astrocytic tissue inhibitor of metalloproteinases-1 drives remyelination

Houben, Evelien; Janssens, Kris; Hermans, Doryssa; Vandooren, Jennifer; Van den Haute, Chris; Schepers, Melissa; Vanmierlo, Tim; Lambrichts, Ivo; van Horssen, Jack; Baekelandt, Veerle

Published in:
Proceedings of the National Academy of Sciences of the United States of America

DOI:
10.1073/pnas.1912910117

Oncostatin M-induced astrocytic tissue inhibitor of metalloproteinases-1 drives remyelination

Evelien Houben[a,1], Kris Janssens[a,1], Doryssa Hermans[a], Jennifer Vandooren[b], Chris Van den Haute[c,d], Melissa Schepers[a,e], Tim Vanmierlo[a,e], Ivo Lambrichts[f], Jack van Horssen[a,g], Veerle Baekelandt[c], Ghislain Opdenakker[b], Wia Baron[h], Bieke Broux[a,1], Helena Slaets[a,1], and Niels Hellings[a,1,2]

[a]Department of Immunology, Biomedical Research Institute, Hasselt University, 3590 Diepenbeek, Belgium; [b]Department of Microbiology and Immunology, Laboratory of Immunobiology, Rega Institute, Katholieke Universiteit (KU) Leuven, 3000 Leuven, Belgium; [c]Department of Neurosciences, Laboratory for Neurobiology and Gene Therapy, KU Leuven, 3000 Leuven, Belgium; [d]Leuven Viral Vector Core, KU Leuven, 3000 Leuven, Belgium; [e]School for Mental Health and Neuroscience, Division Translational Neuroscience, Maastricht University, 6200MD Maastricht, The Netherlands; [f]Department of Morphology, Biomedical Research Institute, Hasselt University, 3590 Diepenbeek, Belgium; [g]Department of Molecular Cell Biology and Immunology, Amsterdam Neuroscience, Amsterdam University Medical Center, location Vrije Universiteit (VU) University Medical Center, Multiple Sclerose Centrum, 1007 MB Amsterdam, The Netherlands; and [h]Section Molecular Neurobiology, Department Biomedical Sciences of Cells and Systems, University Medical Center Groningen, University of Groningen, 9713 AV Groningen, The Netherlands

Edited by Lawrence Steinman, Stanford University School of Medicine, Stanford, CA, and approved January 25, 2020 (received for review July 26, 2019)

The brain's endogenous capacity to restore damaged myelin deteriorates during the course of demyelinating disorders. Currently, no treatment options are available to establish remyelination. Chronic demyelination leads to damaged axons and irreversible destruction of the central nervous system (CNS). We identified two promising therapeutic candidates which enhance remyelination: oncostatin M (OSM), a member of the interleukin-6 family, and downstream mediator tissue inhibitor of metalloproteinases-1 (TIMP-1). While remyelination was completely abrogated in OSMRβ knockout (KO) mice, OSM overexpression in the chronically demyelinated CNS established remyelination. Astrocytic TIMP-1 was demonstrated to play a pivotal role in OSM-mediated remyelination. Astrocyte-derived TIMP-1 drove differentiation of oligodendrocyte precursor cells into mature oligodendrocytes in vitro. In vivo, TIMP-1 deficiency completely abolished spontaneous remyelination, phenocopying OSMRβ KO mice. Finally, TIMP-1 was expressed by human astrocytes in demyelinated multiple sclerosis lesions, confirming the human value of our findings. Taken together, OSM and its downstream mediator TIMP-1 have the therapeutic potential to boost remyelination in demyelinating disorders.

oncostatin M | remyelination | oligodendrocyte precursor cells | astrocytes | tissue inhibitor of metalloproteinases-1

Following a demyelinating event, oligodendrocyte precursor cells (OPCs) proliferate and migrate to the lesion site, where they differentiate into oligodendrocytes and enwrap naked axons with new myelin sheaths (1). This remyelination process restores saltatory conduction, protects axons from degeneration, and resolves functional deficits (2–4). Despite the presence of OPCs in demyelinated lesions, remyelination often fails in (inflammatory) demyelinating disorders such as multiple sclerosis (MS) or following traumatic central nervous system (CNS) injury (5–7). An inhibitory environment in and around the lesion impairs remyelination. It leads to a depletion of OPCs, it decreases OPC migration to the lesion site, and it hampers OPC differentiation into oligodendrocytes. This inhibitory environment is created by the secretory products of CNS resident cells and infiltrated immune cells, expression of inhibitory molecules on denuded axons (8), and changes in the composition of the extracellular matrix (ECM), associated with the formation of a glial scar in chronic lesions (9, 10). Astrocytes and microglia are crucially involved in the formation of mature oligodendrocytes and in the myelination of axons by producing neurotrophic factors (11, 12). The involvement of some proteoglycans as ECM building blocks and matrix metalloproteinases as ECM wreckers has been demonstrated as a key modulatory process of demyelination and remyelination (13). It is clear that a permissive environment is essential to allow robust remyelination. For MS, the most common demyelinating disease, current therapies are aimed at modulating or inhibiting the ongoing immune response to limit autoimmune-mediated demyelination, but fail to directly induce repair. Therefore, those treatments are not effective in progressive MS, where compromised remyelination is prominent, resulting in axonal and neuronal death (14). In that light, there is a high need for treatment strategies that revert the nonpermissive environment to establish the inherent property of the CNS to regenerate. One way to do this is to boost endogenous remyelination-enhancing messenger molecules.

Oncostatin M (OSM) is a first messenger molecule that is produced by microglia, hypertrophic astrocytes, and infiltrated immune cells in demyelinated lesions (15). OSM belongs to the gp130-signaling family and has shown neuroprotective effects in previous studies, including ours. OSM limits neuronal cell death caused by excitotoxicity in vitro and in vivo (16, 17) and promotes neurite outgrowth of primary cortical neurons in vitro (18). Furthermore, following spinal cord injury, OSM treatment reduces lesion size, promotes sprouting of nerve fibers, and induces functional recovery (18). Yet, the role of OSM in remyelination remains elusive.

In this study, the cuprizone model is used as a reproducible and well-characterized mouse model of de- and remyelination

Significance

The loss of myelin around axons is a main pathological hallmark of various neurological diseases. In early disease stages, this myelin sheath is restored through a process called remyelination. Later, remyelination fails and becomes the major driver of disease progression. Despite a clear demand for remyelination-enhancing therapies, the need is currently unmet. Here we present oncostatin M receptor signaling and its downstream effector molecule tissue inhibitor of metalloproteinases-1 as decisive mediators of successful remyelination, providing novel therapeutic opportunities for demyelinating disorders.

Author contributions: E.H., K.J., B.B., H.S., and N.H. designed research; E.H., K.J., D.H., J.V., M.S., T.V., I.L., W.B., and H.S. performed research; C.V.d.H., J.v.H., V.B., G.O., and W.B. contributed new reagents/analytic tools; E.H., K.J., D.H., J.V., W.B., B.B., H.S., and N.H. analyzed data; and E.H., K.J., B.B., H.S., and N.H. wrote the paper.

The authors declare no competing interest.

This article is a PNAS Direct Submission.

[1]E.H., K.J., B.B., H.S., and N.H. contributed equally to this work.

[2]To whom correspondence may be addressed. Email: niels.hellings@uhasselt.be.

This article contains supporting information online at https://www.pnas.org/lookup/suppl/doi:10.1073/pnas.1912910117/-/DCSupplemental.

NEUROSCIENCE

(19). On a cuprizone diet, mature oligodendrocytes are depleted, which induces microgliosis resulting in complete demyelination of the corpus callosum (CC). When cuprizone is omitted from the diet, the CC gradually remyelinates (19). We demonstrate that the OSM-specific receptor subunit beta (OSMRβ) is highly up-regulated during remyelination. In OSMRβ-deficient mice, remyelination is completely absent, whereas CNS-targeted lentiviral (LV)-OSM overexpression boosts remyelination. We identify tissue inhibitor of metalloproteinases-1 (TIMP-1), which is produced by astrocytes, as one of the determining factors involved in OSM-driven remyelination. TIMP-1, present in the secretome of OSM-treated astrocytes, is sufficient to induce in vitro OPC differentiation. Moreover, spontaneous remyelination is abolished in animals lacking TIMP-1. In demyelinated white matter lesions of MS patients, we found expression of TIMP-1 in astrocytes, validating its potential as a target in human disease.

This study uncovers a previously uncharacterized and crucial role for OSMR signaling in remyelination and suggests that OSMR activation and its downstream effector molecule, astrocytic TIMP-1, are promising leads for treating demyelinating disorders, including MS.

Results

OSMR Signaling Is Crucial for Remyelination. To determine the involvement of OSMR signaling in remyelination, we first measured the expression level of *Osmrβ* in the brain of cuprizone-challenged mice (Fig. 1*A*). After 5 wk of cuprizone-induced demyelination, mRNA expression of *Osmrβ* was strongly up-regulated, increasing 5.3-fold (Fig. 1*B*). This enhanced *Osmrβ* expression persisted during remyelination compared to healthy mice (3.3-fold after 1 wk of standard diet) (Fig. 1*B*). To define the functional significance of OSMR up-regulation, OSMRβ knockout (KO) mice were used. Five weeks of cuprizone diet induced demyelination to a similar extent in both wild-type (WT) and OSMRβ KO mice, as evidenced by a strong reduction in myelinated area in the CC (Fig. 1 *C* and *D*). In contrast, while WT mice showed a clear increase in myelinated areas in the CC after 2 wk of remyelination, no significant remyelination was seen in OSMRβ KO mice (Fig. 1 *C* and *D*). In line with this, *Mbp* mRNA expression was strongly up-regulated in WT mice after 1 wk of remyelination, whereas this up-regulation was completely absent in OSMRβ KO mice (*SI Appendix*, Fig. S1*A*). mRNA expression of *Mag* (a later marker of oligodendrocyte maturation) was not significantly different between WT and OSMRβ KO mice (*SI Appendix*, Fig. S1*B*). Taken together, in the absence of OSMR signaling, demyelination after 5 wk of cuprizone diet is not affected, while remyelination is abrogated.

Next, we investigated what happens to the different oligodendrocyte maturation stages during de- and remyelination in the absence of OSMR signaling. Five weeks of cuprizone diet reduced the number of mature oligodendrocytes ($CC1^+$) in the CC of both WT and OSMRβ KO mice (Fig. 1*E*), as cuprizone leads to cell death of oligodendrocytes (19, 20). This depletion of mature oligodendrocytes was accompanied by a strong increase in the number of OPCs ($NG2^+$) in WT mice, while in OSMRβ KO mice this was significantly less (Fig. 1*F*). After 2 wk of remyelination, a robust increase in $CC1^+$ oligodendrocytes was found in WT mice, but not in OSMRβ KO mice (Fig. 1*E*). These results are supported by a significantly lower induction of the oligodendrocyte differentiation gene *Lpar1* (21, 22) during remyelination in OSMRβ KO mice compared to WT mice (Fig. 1*G*).

Taken together, the lack of OSMR signaling results in a decreased induction of OPC numbers following acute demyelination and a reduced number of newly formed mature oligodendrocytes after cuprizone withdrawal, ultimately leading to failure of remyelination.

CNS-Targeted LV-OSM Treatment Induces Remyelination of the Chronically Demyelinated Brain. Since OSMRβ deficiency abrogated remyelination, we next investigated whether OSMR engagement, through therapeutic application of a LV vector expressing OSM (LV-OSM), stimulates remyelination in the context of chronic demyelination, a prominent feature in progressive MS currently not targeted by existing therapies (23). WT mice received a cuprizone diet for 12 wk to induce chronic demyelination, resulting in pronounced depletion of oligodendrocytes and OPCs, thereby limiting the rate of spontaneous remyelination after cuprizone withdrawal (24). LV-OSM, or control LV (LV encoding eGFP; LV-eGFP), was injected in the right striatum after 11 wk of cuprizone diet (Fig. 2*A*). We confirmed overexpression of OSM in both the striatum and CC of the transduced hemisphere using immunohistochemistry (*SI Appendix*, Fig. S2). Up-regulation of *Osmrβ* was also detected in the CC during chronic demyelination and persisted during subsequent LV-OSM–induced remyelination (Fig. 2*B*). LV-OSM–treated animals displayed an enlarged myelinated area in the CC after 2 wk of normal diet consecutive to chronic demyelination (Fig. 2 *C* and *E*, $P = 0.057$ compared to the chronically demyelinated CC at 11 wk of cuprizone diet). For LV-eGFP–treated mice no evident remyelination was seen. In line herewith, CNS-targeted LV-OSM treatment significantly decreased the G ratio evidencing remyelination, while no reduction in G ratio was detected in the LV-eGFP control group (Fig. 2 *D* and *F*). In addition, the number of $CC1^+$ mature oligodendrocytes in the CC significantly increased compared to chronic demyelination (week 11), further reflecting the remyelination-inducing properties of OSM (Fig. 2*G*). Collectively, these results show that CNS-targeted LV-OSM treatment during chronic demyelination increased the number of mature oligodendrocytes and established remyelination.

OSMR Signaling Regulates TIMP-1 Production during Remyelination. To uncover the underlying mechanism of OSM-induced remyelination, downstream mediators of OSMR signaling were investigated. Therefore, we measured mRNA expression of trophic factors (ciliary neurotrophic factor [CNTF], leukemia inhibitory factor [LIF], insulin-like growth factor 1 [IGF1], and TIMP-1), inhibitory molecules (Notch1, Jagged1, leucine rich repeat and Ig domain containing (LINGO)-1), pro- and antiinflammatory cytokines (IL-1β, IL-6, and transforming growth factor beta [TGF-β]), and M1/M2/phagocytosis markers (CD32, CD86, CD206, and Lrp1) in the brain (Fig. 3*A*). *Timp-1*, *Cd32*, *Cd86*, and *Igf-1* mRNA levels were up-regulated after 5 wk of cuprizone diet in WT mice, indicating the involvement during demyelination (*SI Appendix*, Fig. S3). Lower mRNA levels of *Timp-1* were observed in the absence of OSMR signaling after acute demyelination and remyelination, compared to WT mice (Fig. 3*A*). Interestingly, during these conditions, high *Lif* mRNA expression was present, possibly due to compensation mechanisms (25). For the other factors, no differences were observed between OSMRβ KO and WT animals. After chronic demyelination, higher *Timp-1*, *Cd32*, *Cd206*, *Cd86*, *Cntf*, and *Il-1β* mRNA levels were detected in LV-OSM–treated mice in the transduced hemisphere, compared to eGFP-treated mice. For *Timp-1*, *Cd32*, and *Il-1β* also higher expression levels were seen at the region of the CC, in the comparison of LV-OSM–treated with LV-eGFP–treated mice (Fig. 3*A*).

Of the preselected molecules, *Timp-1* was the only gene that was down-regulated in OSMRβ-deficient mice, while increased after triggering of the OSMR with OSM, making it a prime candidate as a downstream mediator of remyelination by OSMR signaling. Therefore, a more detailed mRNA profiling of *Timp-1* was examined to follow its expression pattern during the cuprizone experiments. A strong increase in mRNA expression of *Timp-1* was observed in the brain of WT mice after acute demyelination and persisted during the remyelination phase, while

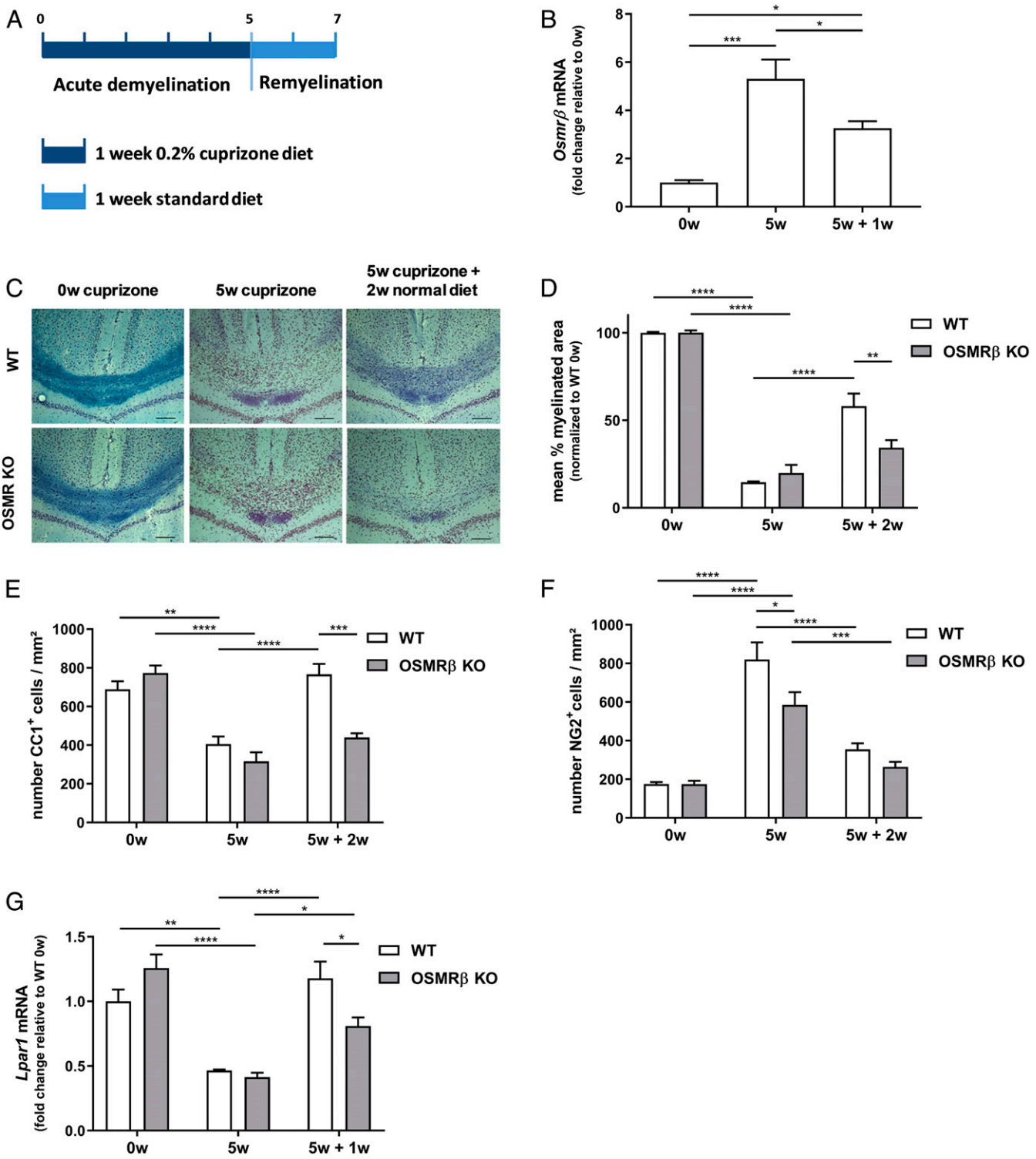

Fig. 1. OSMR signaling is essential for remyelination. (*A*) Mice were fed a 0.2% cuprizone diet for 5 wk to cause demyelination, followed by 2 wk of standard diet to allow spontaneous remyelination. (*B*) *Osmrβ* expression was measured in whole brain of healthy mice, after acute demyelination (5 wk cuprizone diet) and during remyelination (5 wk cuprizone diet followed by 1 wk standard diet) using qPCR ($n = 5$ per group). (*C* and *D*) Representative pictures (*C*) and quantification (*D*) of the Luxol fast blue (LFB) staining in the CC (around bregma −1.82 mm). (*E* and *F*) Number of $CC1^+$ cells (*E*) and $NG2^+$ cells (*F*). All stainings were performed on the CC of WT and OSMRβ KO mice receiving standard diet ($n = 4$ per group), after acute demyelination ($n = 4$ per group), and acute demyelination followed by remyelination ($n = 5$ per group). (*G*) mRNA level of *Lpar1* in whole brain of healthy mice, after acute demyelination (5 wk cuprizone diet) and during remyelination (5 wk cuprizone diet followed by 1 wk standard diet) using qPCR ($n = 5$ per group). Data are depicted as mean ± SEM, $*P < 0.05$, $**P < 0.01$, $***P < 0.001$, and $****P < 0.0001$. One-way ANOVA (*B*) or two-way ANOVA (*D*–*G*) with multiple comparison and Tukey's post hoc test. (Scale bars, 200 μm.)

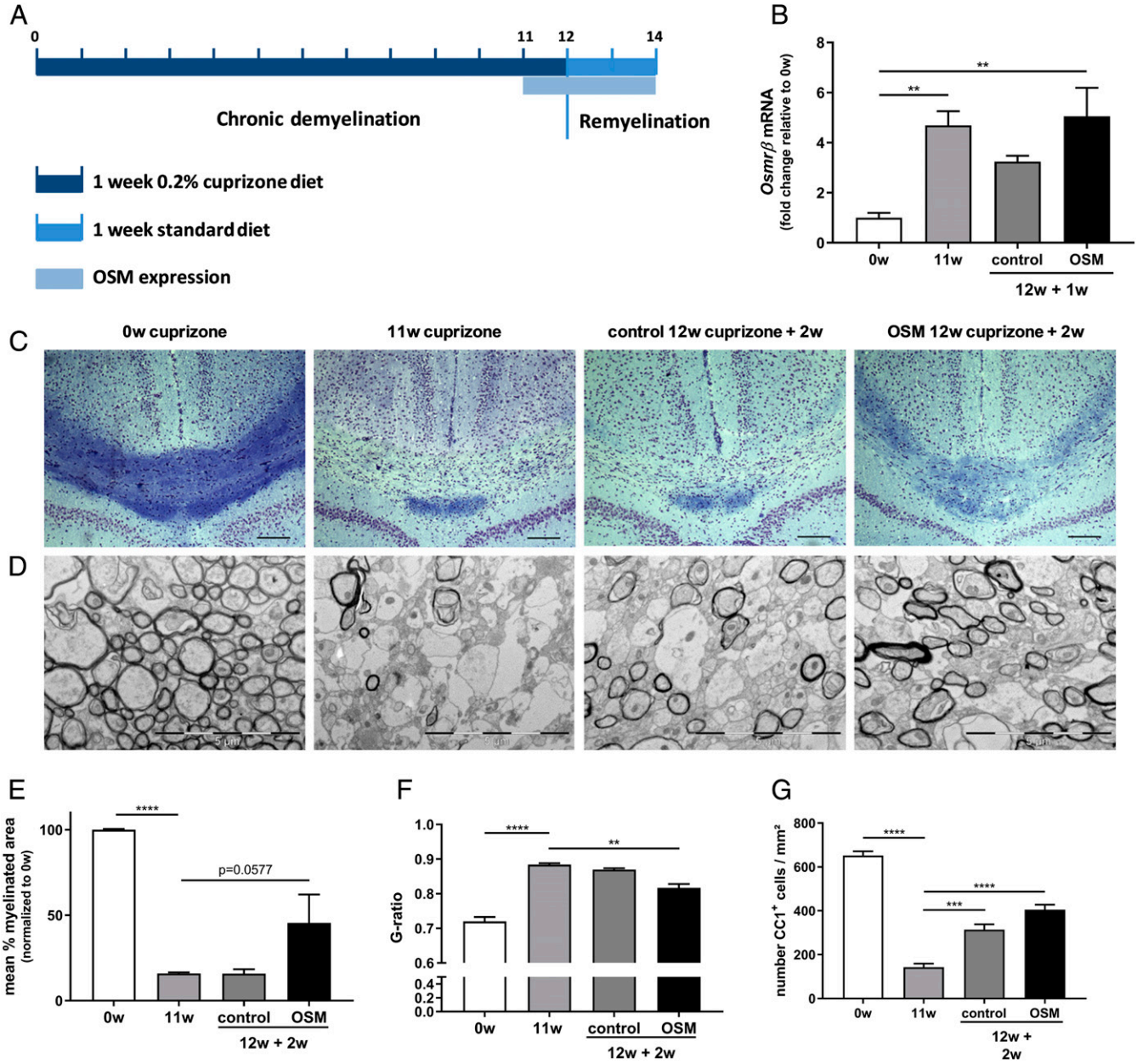

Fig. 2. CNS-targeted OSM treatment enables remyelination after chronic demyelination. (*A*) Schematic representation of cuprizone feeding; mice received cuprizone diet for 12 wk to induce chronic demyelination, followed by 2 wk of standard diet to allow remyelination. After 11 wk, mice were injected with LV-OSM (OSM) or LV-eGFP (control) in the right striatum. (*B*) *OSMRβ* mRNA levels in the CC of healthy mice, after chronic demyelination and during remyelination using qPCR ($n = 5$ per group). (*C* and *E*) Representative images (*C*) and quantification (*E*) of LFB staining in the CC (around bregma −1.82 mm) ($n = 4$ or 5 per group). (*D* and *F*) Representative TEM images (*D*) and quantification of the G ratio (*F*) in the CC ($n = 3$ per group). (*G*) Quantification of $CC1^+$ cells measured using immunohistochemistry in the CC ($n = 4$ or 5 per group). Data are depicted as mean ± SEM, $^{**}P < 0.01$, $^{***}P < 0.001$, and $^{****}P < 0.0001$. One-way ANOVA with multiple comparison and Tukey's post hoc test (*B*) and one-way ANOVA with multiple comparison to 11w and Dunnett's post hoc test (*E–G*). (Scale bars, 200 μm in *C* and 5 μm in *D*.)

in the OSMRβ KO mice—where remyelination is abrogated (Fig. 1 *C* and *D*)—*Timp-1* up-regulation was completely absent (Fig. 3*B*). Moreover, CNS-targeted LV-OSM treatment, enabling remyelination following chronic demyelination, induced a higher *Timp-1* mRNA expression in the region of the CC compared to LV-eGFP control mice (Fig. 3*C*). Since TIMP-1 appears to be the main downstream mediator of OSMR signaling in these models, we also investigated gene expression of *Mmp2* and *Mmp9*, both inhibited by TIMP-1. However, no significant differences were observed for these genes (Fig. 3*A*). Overall, these data point toward an important role for TIMP-1 as a mediator of remyelination downstream of the OSMR, as both endogenous OSMR signaling and LV-OSM treatment strongly regulate its expression.

Astrocytes Produce TIMP-1 in Response to OSM. Next, we sought to identify the cellular source of TIMP-1 in response to OSM. Different cell types of the CNS express OSMRβ, as previously reported by us (26). Moreover, we already identified increased OSMRβ expression in astrocytes and microglia after demyelination using the cuprizone model (26). Most studies assign TIMP-1 expression to astrocytes (27, 28). Therefore, we considered astrocytes to be the main cellular producers of TIMP-1 after

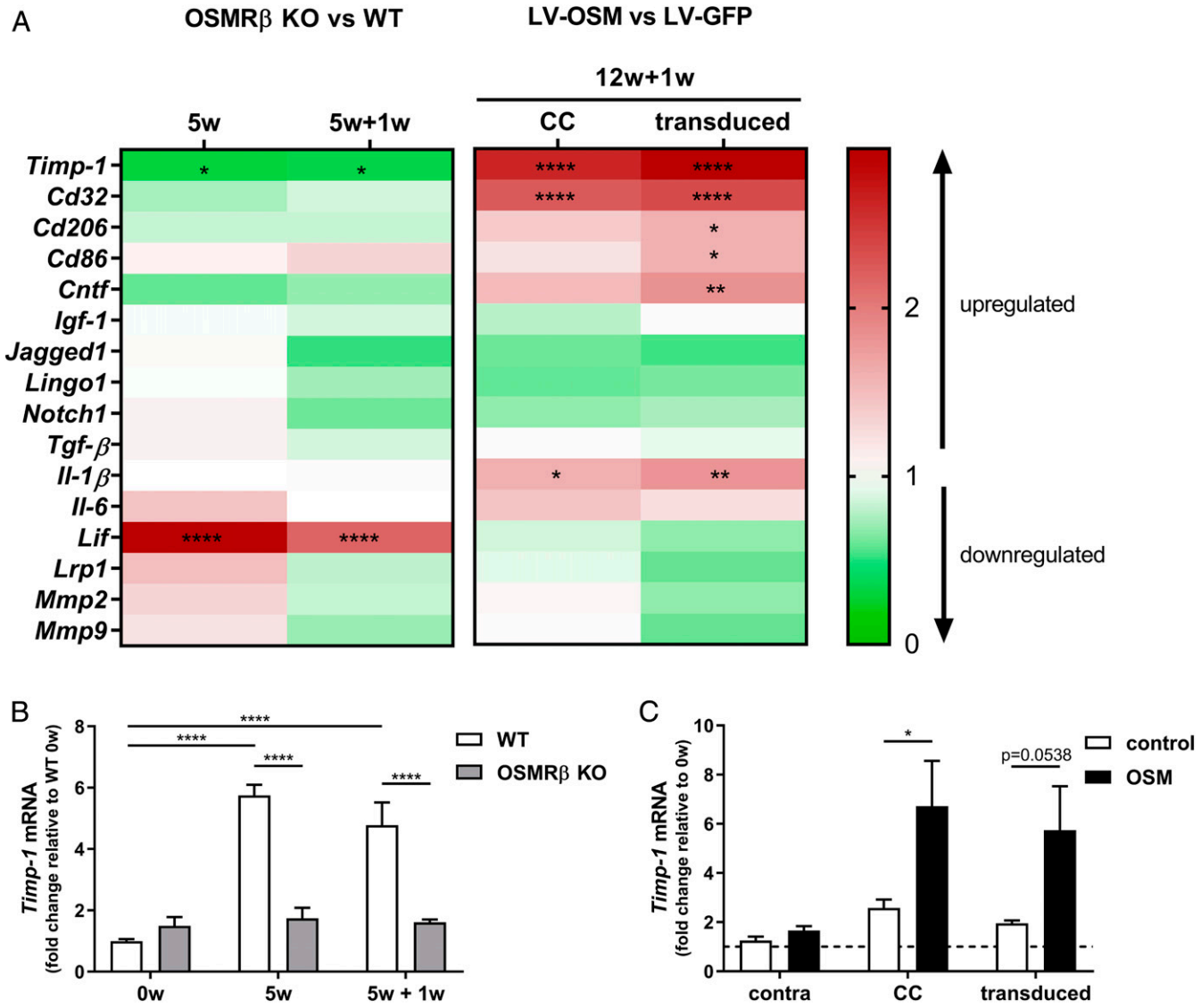

Fig. 3. OSMR signaling induces TIMP-1 production. (*A*) mRNA expression of M1/M2/phagocytosis markers (*Cd32*, *Cd86*, *Cd206*, and *Lrp1*) trophic factors (*Cntf*, *Lif*, *Igf-1*, and *Timp-1*), inhibitory molecules (*Notch1*, *Jagged1*, and *Lingo-1*), pro- and antiinflammatory cytokines (*Il-1β*, *IL-6*, and *Tgf-β*), and matrix metalloproteinases (*Mmp2* and *Mmp9*) measured using qPCR ($n = 5$ per group). Whole brain tissue of OSMRβ KO and WT mice was used after acute demyelination (5 wk cuprizone diet) and following remyelination (5 wk cuprizone diet followed by 1 wk standard diet) (*Left*). For LV-OSM– and LV-eGFP–injected mice during remyelination (12 wk cuprizone followed by 1 wk normal diet), brain tissue in the region of injection (transduced) and region of the CC was used (*Right*). Expression is converted to fold change as compared to WT or LV-eGFP mice, respectively. (*B*) mRNA expression of *Timp-1* in whole brain of WT and OSMRβ KO mice receiving standard diet, after acute demyelination and following remyelination ($n = 5$ per group). (*C*) mRNA expression of *Timp-1* in the region of injection (transduced), contralateral side (contra), and region of the CC in LV-eGFP–(control) and LV-OSM–injected mice (OSM) after 12 wk cuprizone followed by 1 wk normal diet ($n = 5$ per group). Expression is converted to fold change as compared to mice receiving normal diet (dotted line). Data are depicted as mean ± SEM, $^{*}P < 0.05$, $^{**}P < 0.01$, and $^{****}P < 0.0001$. Two-way ANOVA with multiple comparison and Dunnett's post hoc test (*A*), two-way ANOVA with multiple comparison and Tukey's post hoc test (*B*) or Sidak's post hoc test (*C*).

OSMR signaling. Here, we demonstrated that LV-OSM treatment strongly enhanced the astroglial response compared to LV-eGFP controls at the site of injection (Fig. 4 *A* and *B*), though not at the level of the CC (Fig. 4*C*), supporting the active involvement of astrocytes in OSMRβ signaling. Therefore, we investigated whether astrocytes produce TIMP-1 during de- and remyelination. Immunofluorescent double staining in the CC of the LV-OSM–treated mice illustrated coexpression of TIMP-1 with GFAP (Fig. 4*D*). Moreover, treatment of primary cell cultures of astrocytes with recombinant mouse OSM (rmOSM) strongly up-regulated *Timp-1* mRNA levels (Fig. 4*E*). Further validation at the protein level demonstrated expression and a strongly increased secretion of TIMP-1 in primary cultured astrocytes after rmOSM treatment (Fig. 4 *F* and *G*). As expected no TIMP-1 protein levels were detected in astrocyte-conditioned medium (ACM) derived from TIMP-1 KO astrocytes. Taken together, OSMR signaling regulates TIMP-1 production in demyelinating and remyelinating lesions mainly through astrocytes.

Lastly, we analyzed the cellular distribution of TIMP-1 in well-characterized MS lesions (Fig. 5). In control white matter tissue and normal appearing white matter (NAWM), TIMP-1 expression was detected in cells with an astrocytic morphology (Fig. 5*E*). Robust expression of TIMP-1 was observed in the demyelinated white matter (Fig. 5*F*) compared to NAWM (Fig. 5*E*), especially in the active white matter lesion. Double immunohistochemistry revealed that TIMP-1 was markedly expressed in

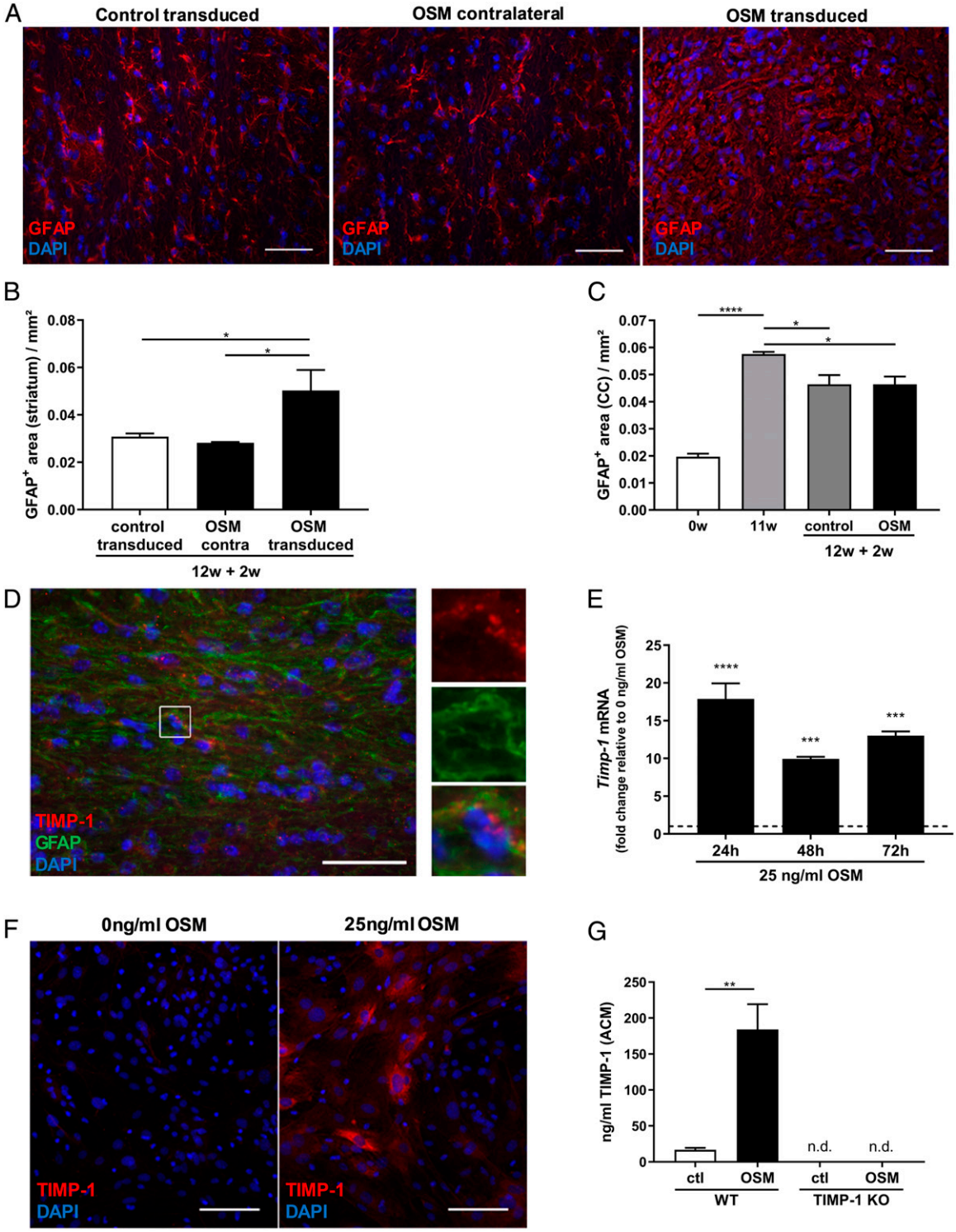

Fig. 4. TIMP-1 is produced by astrocytes after OSM treatment. (*A* and *B*) Representative pictures (*A*) and quantification (*B*) of the GFAP$^+$ area measured at the injection site of control mice (transduced with LV-eGFP), contralateral site of LV-OSM–injected mice (OSM contra) and injection site of LV-OSM–treated mice (transduced with LV-OSM) fed with cuprizone diet for 12 wk followed by 2 wk of standard diet ($n = 4$ or 5 per group). (*C*) Quantification of the GFAP$^+$ area measured using immunohistochemistry in the CC of LV-eGFP– and LV-OSM–treated mice fed with standard diet, cuprizone diet for 11 wk, or cuprizone diet for 12 wk followed by 2 wk of standard diet ($n = 4$ or 5 per group). (*D*) Double immunohistochemical staining for TIMP-1 (red) and GFAP (green) in the CC of the LV-OSM–treated mice following chronic demyelination and remyelination. Magnifications of double positive cells are depicted on the *Right*. (*E*) Primary astrocytes were treated with 0 ng/mL (dashed line) or 25 ng/mL OSM for 24 h, 48 h, and 72 h, after which *Timp-1* mRNA expression was measured by qPCR ($n = 3$). (*F*) Representative pictures of TIMP-1 protein expression in primary astrocytes treated for 72 h with 0 ng/mL or 25 ng/mL rmOSM measured using immunohistochemistry. (*G*) TIMP-1 expression was measured after 72 h OSM treatment in ACM of WT and TIMP-1 KO mice. WT-OSM ACM: 9.6 ± 0.3 ng/mL TIMP-1; WT-no OSM: 1.8 ± 1.3 ng/mL TIMP-1; KO-OSM: not detected (n.d.); KO-no OSM: not detected. Data are depicted as mean ± SEM, $^*P < 0.05$, $^{**}P < 0.01$, $^{***}P < 0.001$, and $^{****}P < 0.0001$. One-way ANOVA with multiple comparison using Tukey's post hoc test (*B* and *C*) or Sidak's post hoc test (*G*). One-way ANOVA with multiple comparison to 0 ng/mL OSM (*E*) and Tukey's post hoc test. (Scale bar, 50 μm.)

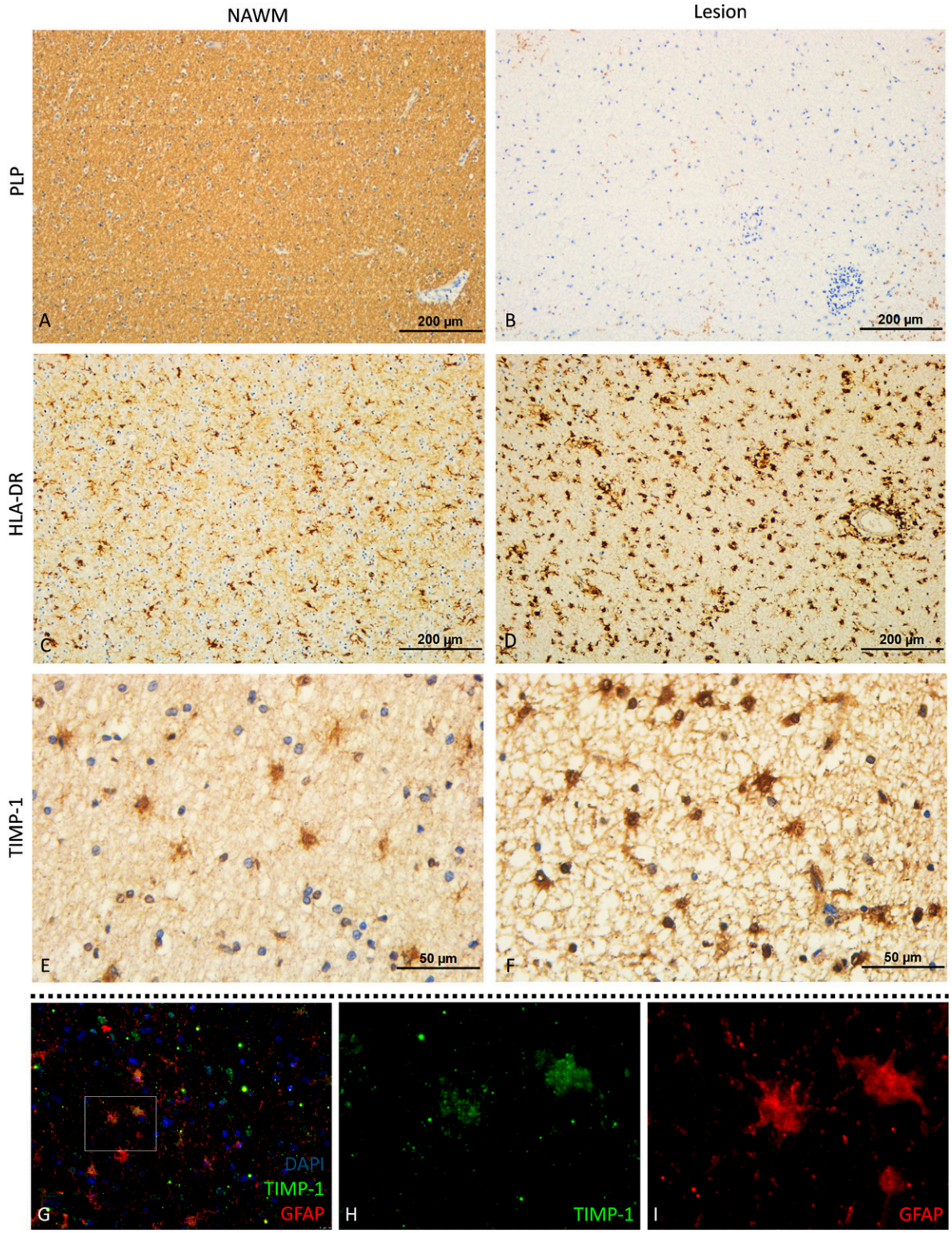

Fig. 5. Astrocytes express TIMP-1 in demyelinated white matter MS lesions. (*A–D*) Classification of the type of MS lesion was done based on proteolipid protein (PLP) (*A* and *B*) and human leukocyte antigen (HLA)-DR (*C* and *D*) staining. (*E* and *F*) TIMP-1 positive cells with an astrocytic morphology are found in NAWM (*E*) as well as in white matter lesions (*F*). (*G–I*) Colocalization of TIMP-1 and GFAP is found in astrocytes.

20 to 58% of all GFAP-positive astrocytes in white matter MS lesions (Fig. 5 *G–I*). These results validate our mouse data, where TIMP-1 expression was attributed to astrocytes and up-regulated after demyelination of the white matter.

TIMP-1 Enhances OPC Differentiation and Is Essential for In Vivo Remyelination. To confirm that OSM-induced astrocytic TIMP-1 is a primary mechanism to induce remyelination, OPCs were incubated for 3 d with ACM derived from WT and TIMP-1 KO

astrocytes treated with or without rmOSM. ACM from OSM-treated WT astrocytes enhanced OPC differentiation compared to ACM from untreated WT astrocytes (Fig. 6*A*). Moreover, ACM from TIMP-1 KO astrocytes, regardless of OSM treatment, did not augment OPC differentiation (Fig. 6*A*). In line herewith, in vitro stimulation of primary OPCs with recombinant rTIMP-1 demonstrated that TIMP-1 directly boosts OPC differentiation after 3 d of stimulation (Fig. 6*B*). This effect was diminished after 6 d of treatment (Fig. 6*B*), indicating accelerated formation of MBP^+ mature OLG by TIMP-1.

Next, the kinetics of TIMP-1 expression and its receptor CD63 were assessed in whole brain during the acute cuprizone model (Fig. 6 *C* and *D*). Both TIMP-1 and CD63 showed highest expression at the peak of demyelination and remained elevated during the remyelination phase. To define whether TIMP-1 deficiency affects remyelination in vivo, TIMP-1 KO mice and WT mice were challenged with cuprizone for 5 wk followed by 2 wk of normal diet (Fig. 1*A*). The expression level of *Cd63*, the cellular receptor for TIMP-1 (29), was significantly up-regulated after 5 wk of cuprizone diet in the CC of both TIMP-1 KO and WT mice. This is indicative of active involvement of TIMP-1 signaling in acutely demyelinated regions (Fig. 6*E*). No compensatory expression of the other TIMP family members (TIMP-2, -3, and -4) was detected after deletion of TIMP-1 (*SI Appendix*, Fig. S4). In agreement with the strong up-regulation of the OSMR during cuprizone-induced de- and remyelination, *Osmrβ* was also significantly up-regulated after 5 wk of cuprizone exposure in the CC of TIMP-1 KO mice (Fig. 6*F*). Demyelination was induced to a similar extent in both WT and TIMP-1 KO mice after 5 wk of cuprizone treatment (Fig. 6 *G* and *H*). In contrast, after 2 wk of standard chow, significant remyelination was seen in WT, but significantly less in TIMP-1 KO mice (Fig. 6 *G* and *H*). In conclusion, we directly linked OSM-induced astrocytic TIMP-1 production to enhanced OPC differentiation. Moreover, our results in TIMP-1 KO mice phenocopied the findings in OSMR KO mice, identifying TIMP-1 as a major effector molecule of OSM-mediated remyelination.

Discussion

In this study, we identified OSMR signaling and its effector molecule TIMP-1 as essential mediators for remyelination. First, we demonstrated that OSMRβ was up-regulated during remyelination. Expression of OSM and its receptor are increased in response to different types of CNS pathology, such as nerve injury, epileptic seizures, spinal cord injury, and MS (15, 18, 30, 31). Whereas these studies pointed to a direct neuroprotective effect of OSM, this study shows that OSMR signaling is essential for remyelination. In OSMRβ KO mice, OPC numbers were reduced in the CC following acute demyelination compared to WT, coinciding with a decrease in newly formed oligodendrocytes and subsequent failure of remyelination. A possible explanation could be that the OPCs lose the ability to fully develop into myelinating oligodendrocytes when OSMRβ signaling is absent. Of course we cannot exclude the involvement of OSMRβ signaling in other mechanisms such as reduced cell survival. In contrast, CNS-targeted LV-OSM treatment following chronic demyelination enhanced the number of newly formed mature oligodendrocytes in the CC, thereby enabling remyelination.

To investigate the underlying mechanism of OSM-induced remyelination, different candidate downstream mediators were investigated. In the absence of OSMR signaling, LIF expression was increased during de- and remyelination. A compensatory mechanism due to the shared gp130 subunit for the OSMR and LIF receptor (LIFR) (25) is credible. LIF was previously reported by us and others to protect OPCs and oligodendrocytes from inflammation-induced cell death (32–35). At the site of OSM overexpression higher levels of neurotrophic factor CNTF, proinflammatory (CD86 and IL1β), and antiinflammatory (CD32 and CD206) mediators were detected, all known to promote remyelination (36–39). Yet, TIMP-1 was the only factor both reduced in the absence of OSMRβ and increased upon LV-OSM treatment. Here, we identify TIMP-1 as one of the major effector molecules responsible for OSMR signaling-induced remyelination. As remyelination is a highly complex process, we do not exclude the involvement of other mediators (40, 41).

In response to demyelination, TIMP-1 expression is robustly induced in line with previous reports (28, 42–44). Here we demonstrate that in the absence of OSMRβ, up-regulation of TIMP-1 is abrogated, indicating the crucial role of endogenous OSMR signaling to induce TIMP-1 in demyelinated lesions. Moreover, CNS-targeted LV-OSM treatment strongly increased TIMP-1 expression and reinstalled remyelination. Finally, we demonstrated that TIMP-1 deficiency phenocopied the abrogation of remyelination in OSMRβ KO mice. Thus, both OSMR signaling as well as its downstream mediator TIMP-1 are essential for remyelination. Astrocytes were major producers of TIMP-1 in our model, and express a functional OSMR (26, 45). While we cannot exclude other sources of TIMP-1, there is ample evidence from other studies confirming our findings in demyelinated lesions (27, 28, 42, 46). Accumulating evidence indicates that astrocytes are key players in CNS repair (11, 47) in addition to earlier reported neuroinflammation-promoting characteristics (48). They are the most abundant cell type in the CNS and fulfill multiple functions such as maintaining metabolic homeostasis, regulation of synaptogenesis, formation of the blood–brain barrier, and providing trophic support. Following CNS damage, astrocytes produce factors that promote OPC proliferation, differentiation, and myelination (47, 49, 50). In this study, CNS-targeted LV-OSM expression induced a local astroglial reaction at the site of overexpression. TIMP-1 expression was evident in the accumulating astrocytes and we confirmed that rmOSM directly induced TIMP-1 production in primary astrocytes. Taken together, our data support the notion that astrocytes play an essential role during remyelination through OSM-induced TIMP-1 production.

Importantly, we identified a direct link between OSM and astrocytic TIMP-1 on OPC differentiation. The secretome of OSM-treated astrocytes enhanced OPC differentiation, while this effect was not observed with the secretome of OSM-treated TIMP-1 KO astrocytes. Moreover, our in vitro experiments show that TIMP-1 directly accelerated OPC differentiation, in line with results obtained by Moore et al. (51), again underscoring the involvement of TIMP-1 in the remyelination process. TIMP-1 may establish remyelination through different mechanisms. TIMP-1 is an endogenous regulator of the proteolytic action of matrix metalloproteinases (MMPs) (52, 53), which are important to create a remyelination-permissive environment via modulation of the ECM (13, 54, 55). The MMP-dependent function of TIMP-1 is therefore definitely important. Since ECM components were not exogenously added to our assays, this suggests that a second mechanism, related to the less characterized MMP-independent functions of TIMP-1 (56), particularly contributes to the effects we observed. Moreover, a recent report described no effect of a broad spectrum MMP inhibitor on OPC differentiation. Yet, OPC differentiation could be induced with the C-terminal domain of TIMP-1 (57), which is essential for MMP-independent TIMP-1 signaling via the CD63/β1 receptor (29). In line with this, we found robust up-regulation of CD63 in acutely demyelinated regions, indicating that this pathway is active in our in vivo model. These findings suggest that CD63/β1 signaling is heavily involved in TIMP-1–induced OPC differentiation in vitro. In addition, we now report an increase of astrocytic TIMP-1 expression in human white matter MS lesions, warranting its use for human applications.

Since OSM signals through both the OSMR and LIFR in humans (58, 59), the effects of LIFR activation also need to be taken into consideration when designing new therapeutic strategies based on the findings reported here. LIFR signaling influences the

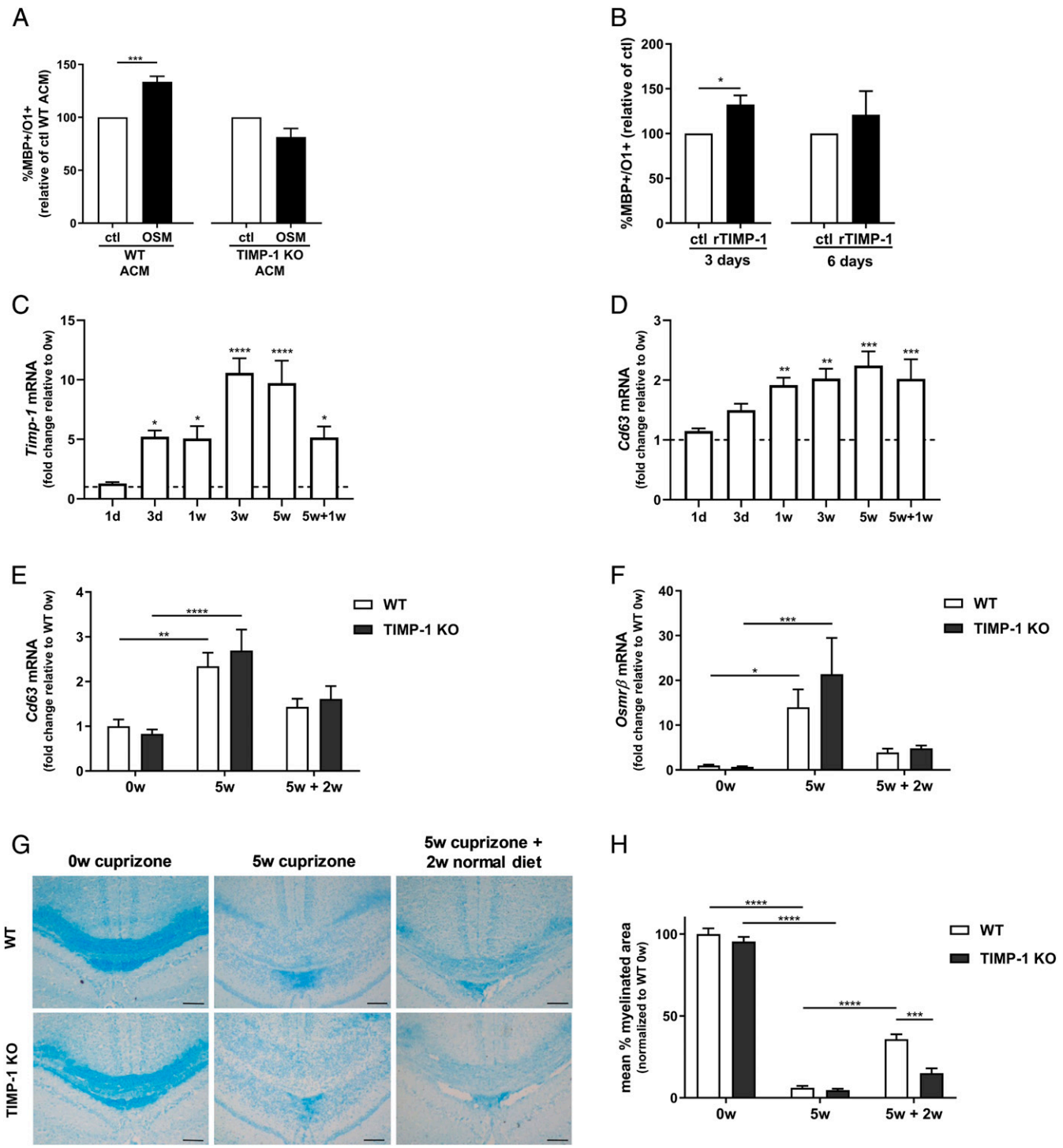

Fig. 6. TIMP-1 is crucial for in vitro OPC differentiation and in vivo remyelination. (*A* and *B*) Ratio of MBP$^+$ oligodendrocytes and O1$^+$ cells to quantify OPC differentiation into mature oligodendrocytes after 3 d of incubation with ACM from WT ($n = 10$) and TIMP-1 KO ($n = 4$) astrocytes treated with or without rmOSM (*A*) or after 3 d ($n = 4$) and 6 d ($n = 3$) of 10 ng/mL recombinant rTIMP-1 treatment (*B*). (*C* and *D*) *Timp-1* (*C*) and *Cd63* (*D*) mRNA levels in whole brain of healthy mice, during acute demyelination and remyelination ($n = 5$ per group). (*E* and *F*) mRNA expression of *Cd63* (*E*) and *OSMRβ* (*F*) in the CC of naive WT and TIMP-1 KO mice and after de- and remyelination. (*G* and *H*) Representative pictures (*G*) and quantification (*H*) of the myelinated area measured using LFB staining in the CC (around bregma −1.82 mm) in WT and TIMP-1 KO mice receiving a normal diet ($n = 5$ or 6 per group) or a cuprizone diet for 5 wk ($n = 5$ per group) and 5 wk followed by 2 wk normal diet (WT $n = 5$; KO $n = 6$). Data are depicted as mean ± SEM, $^*P < 0.05$, $^{**}P < 0.01$, $^{***}P < 0.001$, and $^{****}P < 0.0001$. One-sample *t* test (*A* and *B*), one-way ANOVA with multiple comparisons to 0w (dotted line) and Dunnett's post hoc test (*C* and *D*), two-way ANOVA with multiple comparison and Tukey's post hoc test (*F*) or with multiple comparison to 0w and Dunnett's post hoc test (*C* and *D*). (Scale bars, 200 μm.)

Th17/Treg axis toward Treg expansion and thereby promotes immune tolerance (60, 61). Moreover, protective effects of LIF on neural survival are already described (32–34, 62). Therefore, stimulation of endogenous pathways through both the OSMR and LIFR has promising implications for the clinic. The main reason for using mouse models was to discriminate OSM actions specifically related to OSMR ligation from those related to LIFR signaling, as mouse OSM selectively binds to OSMR in contrast to what is seen in the human situation (63). Taken together, we identify the crucial role of OSMR signaling, as well as its downstream mediator TIMP-1, in promoting remyelination. Together with the reported well-established neuroprotective properties, OSM and TIMP-1 are promising therapeutic candidates for demyelinating CNS disorders.

Materials and Methods

For the materials and methods used in this study, a detailed description is available in *SI Appendix*, including: experimental setup, cuprizone and lentiviral vector treatment, cell culture of primary astrocytes and oligodendrocyte precursor cells, ELISA, histochemistry, immunocytochemistry, quantitative PCR, transmission electron microscopy (TEM), and statistical analysis. All animal procedures were in accordance with the EU directive 2010/63/EU, and all mouse experiments were approved by the Hasselt University Ethics Committee for Animal Experiments. All rat experiments were approved by the Institutional Animal Care and Use Committee of the University of Groningen.

Data Availability Statement. All relevant data are within the manuscript and *SI Appendix*.

ACKNOWLEDGMENTS. We thank Dr. Tom Struys, Katrien Wauterickx, and Joke Vanhoof for excellent technical assistance. This work was financially supported by grants from the Research Foundation of Flanders (FWO Vlaanderen, G04441N, G050617N, G0A5716N, and 1106817N), the Interuniversity Attraction Poles (IUAP-P7-39), the Belgian MS-Liga and the Charcot Foundation of Belgium, Methusalem NEURONET, the European FP7 project, HEALTH-F2-2011-278850 (INMiND), and Bijzonder Onderzoeksfonds (BOF)-UHasselt.

1. R. J. Franklin, C. Ffrench-Constant, Remyelination in the CNS: From biology to therapy. *Nat. Rev. Neurosci.* **9**, 839–855 (2008).
2. K. J. Smith, W. F. Blakemore, W. I. McDonald, Central remyelination restores secure conduction. *Nature* **280**, 395–396 (1979).
3. K. A. Irvine, W. F. Blakemore, Remyelination protects axons from demyelination-associated axon degeneration. *Brain* **131**, 1464–1477 (2008).
4. N. D. Jeffery, W. F. Blakemore, Locomotor deficits induced by experimental spinal cord demyelination are abolished by spontaneous remyelination. *Brain* **120**, 27–37 (1997).
5. N. Scolding *et al*., Oligodendrocyte progenitors are present in the normal adult human CNS and in the lesions of multiple sclerosis. *Brain* **121**, 2221–2228 (1998).
6. A. Chang, A. Nishiyama, J. Peterson, J. Prineas, B. D. Trapp, NG2-positive oligodendrocyte progenitor cells in adult human brain and multiple sclerosis lesions. *J. Neurosci.* **20**, 6404–6412 (2000).
7. Y. Maeda *et al*., Platelet-derived growth factor-alpha receptor-positive oligodendroglia are frequent in multiple sclerosis lesions. *Ann. Neurol.* **49**, 776–785 (2001).
8. M. Podbielska, N. L. Banik, E. Kurowska, E. L. Hogan, Myelin recovery in multiple sclerosis: The challenge of remyelination. *Brain Sci.* **3**, 1282–1324 (2013).
9. A. O. Dulamea, The contribution of oligodendrocytes and oligodendrocyte progenitor cells to central nervous system repair in multiple sclerosis: Perspectives for remyelination therapeutic strategies. *Neural Regen. Res.* **12**, 1939–1944 (2017).
10. T. Philips, J. D. Rothstein, Oligodendroglia: Metabolic supporters of neurons. *J. Clin. Invest.* **127**, 3271–3280 (2017).
11. S. C. Barnett, C. Linington, Myelination: Do astrocytes play a role? *Neuroscientist* **19**, 442–450 (2013).
12. X. Hu *et al*., Microglial and macrophage polarization—New prospects for brain repair. *Nat. Rev. Neurol.* **11**, 56–64 (2015).
13. P. H. Larsen, J. E. Wells, W. B. Stallcup, G. Opdenakker, V. W. Yong, Matrix metalloproteinase-9 facilitates remyelination in part by processing the inhibitory NG2 proteoglycan. *J. Neurosci.* **23**, 11127–11135 (2003).
14. D. H. Mahad, B. D. Trapp, H. Lassmann, Pathological mechanisms in progressive multiple sclerosis. *Lancet Neurol.* **14**, 183–193 (2015).
15. K. Ruprecht *et al*., Effects of oncostatin M on human cerebral endothelial cells and expression in inflammatory brain lesions. *J. Neuropathol. Exp. Neurol.* **60**, 1087–1098 (2001).
16. T. W. Weiss, A. L. Samson, B. Niego, P. B. Daniel, R. L. Medcalf, Oncostatin M is a neuroprotective cytokine that inhibits excitotoxic injury in vitro and in vivo. *FASEB J.* **20**, 2369–2371 (2006).
17. S. Moidunny *et al*., Interleukin-6-type cytokines in neuroprotection and neuromodulation: Oncostatin M, but not leukemia inhibitory factor, requires neuronal adenosine A1 receptor function. *J. Neurochem.* **114**, 1667–1677 (2010).
18. H. Slaets *et al*., Oncostatin M reduces lesion size and promotes functional recovery and neurite outgrowth after spinal cord injury. *Mol. Neurobiol.* **50**, 1142–1151 (2014).
19. G. K. Matsushima, P. Morell, The neurotoxicant, cuprizone, as a model to study demyelination and remyelination in the central nervous system. *Brain Pathol.* **11**, 107–116 (2001).
20. P. Acs *et al*., 17beta-estradiol and progesterone prevent cuprizone provoked demyelination of corpus callosum in male mice. *Glia* **57**, 807–814 (2009).
21. P. Cervera *et al*., Immunohistological localization of the myelinating cell-specific receptor LP(A1). *Glia* **38**, 126–136 (2002).
22. J. C. Dugas, Y. C. Tai, T. P. Speed, J. Ngai, B. A. Barres, Functional genomic analysis of oligodendrocyte differentiation. *J. Neurosci.* **26**, 10967–10983 (2006).
23. H. Lassmann, M. Bradl, Multiple sclerosis: Experimental models and reality. *Acta Neuropathol.* **133**, 223–244 (2017).
24. J. L. Mason *et al*., Oligodendrocytes and progenitors become progressively depleted within chronically demyelinated lesions. *Am. J. Pathol.* **164**, 1673–1682 (2004).
25. S. H. Chen, E. N. Benveniste, Oncostatin M: A pleiotropic cytokine in the central nervous system. *Cytokine Growth Factor Rev.* **15**, 379–391 (2004).
26. K. Janssens *et al*., Oncostatin M protects against demyelination by inducing a protective microglial phenotype. *Glia* **63**, 1729–1737 (2015).
27. H. Toft-Hansen, R. K. Nuttall, D. R. Edwards, T. Owens, Key metalloproteinases are expressed by specific cell types in experimental autoimmune encephalomyelitis. *J. Immunol.* **173**, 5209–5218 (2004).
28. J. Skuljec *et al*., Matrix metalloproteinases and their tissue inhibitors in cuprizone-induced demyelination and remyelination of brain white and gray matter. *J. Neuropathol. Exp. Neurol.* **70**, 758–769 (2011).
29. J. Kobuch *et al*., TIMP-1 signaling via CD63 triggers granulopoiesis and neutrophilia in mice. *Haematologica* **100**, 1005–1013 (2015).
30. Y. Ito *et al*., Temporal expression of mRNAs for neuropoietic cytokines, interleukin-11 (IL-11), oncostatin M (OSM), cardiotrophin-1 (CT-1) and their receptors (IL-11Ralpha and OSMRbeta) in peripheral nerve injury. *Neurochem. Res.* **25**, 1113–1118 (2000).
31. J. L. Jankowsky, P. H. Patterson, Differential regulation of cytokine expression following pilocarpine-induced seizure. *Exp. Neurol.* **159**, 333–346 (1999).
32. H. Slaets *et al*., CNS-targeted LIF expression improves therapeutic efficacy and limits autoimmune-mediated demyelination in a model of multiple sclerosis. *Mol. Ther.* **18** 684–691 (2010).
33. J. Vanderlocht *et al*., Leukemia inhibitory factor is produced by myelin-reactive T cells from multiple sclerosis patients and protects against tumor necrosis factor-alpha-induced oligodendrocyte apoptosis. *J. Neurosci. Res.* **83**, 763–774 (2006).
34. H. Butzkueven *et al*., LIF receptor signaling limits immune-mediated demyelination by enhancing oligodendrocyte survival. *Nat. Med.* **8**, 613–619 (2002).
35. S. Rittchen *et al*., Myelin repair in vivo is increased by targeting oligodendrocyte precursor cells with nanoparticles encapsulating leukaemia inhibitory factor (LIF). *Biomaterials* **56**, 78–85 (2015).
36. J. L. Mason, K. Suzuki, D. D. Chaplin, G. K. Matsushima, Interleukin-1β promotes repair of the CNS. *J. Neurosci.* **21**, 7046–7052 (2001).
37. T. Tanaka, K. Murakami, Y. Bando, S. Yoshida, Minocycline reduces remyelination by suppressing ciliary neurotrophic factor expression after cuprizone-induced demyelination. *J. Neurochem.* **127**, 259–270 (2013).
38. L. A. Peferoen *et al*., Activation status of human microglia is dependent on lesion formation stage and remyelination in multiple sclerosis. *J. Neuropathol. Exp. Neurol.* **74**, 48–63 (2015).
39. K. Zhu *et al*., Electroacupuncture promotes remyelination after cuprizone treatment by enhancing myelin debris clearance. *Front. Neurosci.* **10**, 613 (2017).
40. B. Stankoff *et al*., Ciliary neurotrophic factor (CNTF) enhances myelin formation: A novel role for CNTF and CNTF-related molecules. *J. Neurosci.* **22**, 9221–9227 (2002).
41. S. Mi *et al*., LINGO-1 antagonist promotes spinal cord remyelination and axonal integrity in MOG-induced experimental autoimmune encephalomyelitis. *Nat. Med.* **13**, 1228–1233 (2007).
42. A. Pagenstecher, A. K. Stalder, C. L. Kincaid, S. D. Shapiro, I. L. Campbell, Differential expression of matrix metalloproteinase and tissue inhibitor of matrix metalloproteinase genes in the mouse central nervous system in normal and inflammatory states. *Am. J. Pathol.* **152**, 729–741 (1998).
43. S. J. Crocker *et al*., Persistent macrophage/microglial activation and myelin disruption after experimental autoimmune encephalomyelitis in tissue inhibitor of metalloproteinase-1-deficient mice. *Am. J. Pathol.* **169**, 2104–2116 (2006).
44. R. Ulrich *et al*., MMP-12, MMP-3, and TIMP-1 are markedly upregulated in chronic demyelinating theiler murine encephalomyelitis. *J. Neuropathol. Exp. Neurol.* **65**, 783–793 (2006).
45. M. P. Hsu, R. Frausto, S. Rose-John, I. L. Campbell, Analysis of IL-6/gp130 family receptor expression reveals that in contrast to astroglia, microglia lack the oncostatin M receptor and functional responses to oncostatin M. *Glia* **63**, 132–141 (2015).
46. P. T. Nygårdas, A. E. Hinkkanen, Up-regulation of MMP-8 and MMP-9 activity in the BALB/c mouse spinal cord correlates with the severity of experimental autoimmune encephalomyelitis. *Clin. Exp. Immunol.* **128**, 245–254 (2002).
47. C. S. Moore, S. L. Abdullah, A. Brown, A. Arulpragasam, S. J. Crocker, How factors secreted from astrocytes impact myelin repair. *J. Neurosci. Res.* **89**, 13–21 (2011).
48. E. Colombo, C. Farina, Astrocytes: Key regulators of neuroinflammation. *Trends Immunol.* **37**, 608–620 (2016).

49. R. H. Woodruff, M. Fruttiger, W. D. Richardson, R. J. Franklin, Platelet-derived growth factor regulates oligodendrocyte progenitor numbers in adult CNS and their response following CNS demyelination. *Mol. Cell. Neurosci.* **25**, 252–262 (2004).
50. T. Ishibashi *et al*., Astrocytes promote myelination in response to electrical impulses. *Neuron* **49**, 823–832 (2006).
51. C. S. Moore *et al*., Astrocytic tissue inhibitor of metalloproteinase-1 (TIMP-1) promotes oligodendrocyte differentiation and enhances CNS myelination. *J. Neurosci.* **31**, 6247–6254 (2011).
52. G. Murphy, Tissue inhibitors of metalloproteinases. *Genome Biol.* **12**, 233 (2011).
53. M. Shimoda *et al*., Loss of the Timp gene family is sufficient for the acquisition of the CAF-like cell state. *Nat. Cell Biol.* **16**, 889–901 (2014).
54. P. Wang *et al*., MMP7 cleaves remyelination-impairing fibronectin aggregates and its expression is reduced in chronic multiple sclerosis lesions. *Glia* **66**, 1625–1643 (2018).
55. J. M. Stoffels, D. Hoekstra, R. J. Franklin, W. Baron, C. Zhao, The EIIIA domain from astrocyte-derived fibronectin mediates proliferation of oligodendrocyte progenitor cells following CNS demyelination. *Glia* **63**, 242–256 (2015).
56. C. Ashutosh, C. Chao, K. Borgmann, K. Brew, A. Ghorpade, Tissue inhibitor of metalloproteinases-1 protects human neurons from staurosporine and HIV-1-induced apoptosis: Mechanisms and relevance to HIV-1-associated dementia. *Cell Death Dis.* **3**, e332 (2012).
57. A. M. Nicaise, K. M. Johnson, C. M. Willis, R. M. Guzzo, S. J. Crocker, TIMP-1 promotes oligodendrocyte differentiation through receptor-mediated signaling. *Mol. Neurobiol.* **56**, 3380–3392 (2018).
58. D. P. Gearing *et al*., The IL-6 signal transducer, gp130: an oncostatin M receptor and affinity converter for the LIF receptor. *Science* **255**, 1434–1437 (1992).
59. B. Thoma, T. A. Bird, D. J. Friend, D. P. Gearing, S. K. Dower, Oncostatin M and leukemia inhibitory factor trigger overlapping and different signals through partially shared receptor complexes. *J. Biol. Chem.* **269**, 6215–6222 (1994).
60. J. Park *et al*., Modulation of CD4+ T lymphocyte lineage outcomes with targeted, nanoparticle-mediated cytokine delivery. *Mol. Pharm.* **8**, 143–152 (2011).
61. W. Gao *et al*., Treg versus Th17 lymphocyte lineages are cross-regulated by LIF versus IL-6. *Cell Cycle* **8**, 1444–1450 (2009).
62. S. M. Davis *et al*., Leukemia inhibitory factor protects neurons from ischemic damage via upregulation of superoxide dismutase 3. *Mol. Neurobiol.* **54**, 608–622 (2017).
63. M. Ichihara, T. Hara, H. Kim, T. Murate, A. Miyajima, Oncostatin M and leukemia inhibitory factor do not use the same functional receptor in mice. *Blood* **90**, 165–173 (1997).